PNC TN941 80-131

LOCAL TEMPERATURE RISE AND BOILING BEHAVIOR BEHIND A CENTRAL BLOCKAGE IN A WIRE-WRAPPED PIN BUNDLE

August, 1 9 8 0

Power Reactor and Nuclear Fuel Development Corporation

PNC TN941 80－131

Aug., 1980

Paper presented to the 9th Liquid Metal Boiling Working Group Meeting

June 4－6, 1980
Rome, Italy

LOCAL TEMPERATURE RISE AND BOILING BEHAVIOR BEHIND A CENTRAL BLOCKAGE IN A WIRE-WRAPPED PIN BUNDLE

K. Yamaguchi*, M. Uotani*, K. Haga* and M. Hori*

O-arai Engineering Center, Power Reactor
and Nuclear Fuel Development Corporation, Japan

ABSTRACT

The succeeding series of central-type blockage experiments were completed by the present one with 61-pin bundle test section. The interpretations of the present test results and those of our previous bundle configurations were summarized in the present paper.

Concerning the single-phase flow, an empirical formula was derived to estimate the temperature rises behind various central-type blockages: $\tau U_B/d_h = 35.3(D_B/p)^{0.85}$, where $\tau U_B/d_h$ is the dimensionless residence time and D_B/p is the Ring Parameter newly introduced here. This formula was validated to be effective within the region up to x4 mockup scale ($3.0 \leq d_h \leq 16.1$ mm) and was also supported by the data of KfK and ORNL. It was guessed that the apparent peaking factor of temperature rises in the wake region that would be observed in case of bare bundle was about 1.5 and that the effect of three-dimensional distortion due to spacer wires was from 0.9 to 1.2. The estimation of peak temperature rise by the present formula and two kinds of constants led the conclusion that the central-type blockage will not cause local boiling without being detected by an in-core flow-meter.

In case of sodium boiling two-phase flow, existence of a large boiling window could be identified through the experimental knowledge on oscillatory boiling and dry-out mechanism: the stable oscillatory behavior of a single bubble (or a cluster of bubbles) was never terminated untill the saturated region being widely built up enough to yeild the one-sided expansion of bubbly region and following clad melting. The oscillation improved the mass exchange between localized bubbly region and surrounding subcooled free stream region in compared with that under non-oscillatory conditions, and often relieved clads from melting.

INTRODUCTION

In the current safety research of an LMFBR, the formation of local flow blockage has been treated as one of the possible initiator of fuel failure propagation in a subassembly. In the present paper, we deal with the early two stages in the event tree in question:

(1) the estimation method of temperature field behind the blockage, which results in the conditions of the onset of sodium boiling;
(2) the critical conditions of the occurrence of local clad melting followed by local dry-out of pin surfaces.

EXPERIMENTAL EQUIPMENT AND OPERATING PROCEDURES

Test Section

A series of experiments were carried out with the Sodium Boiling and Fuel Failure Propagation Tesst Facility SIENA in FBR Safety Section of OEC/PNC.

Figure 1 shows a sketch of the locally blocked 61-pin bundle wire-spacer type test section. In order to simulate an LMFBR fuel subassembly, a total of 61-pin bundle was installed in a hexagonal tube of 64.1 mm inside flat-to-flat distance. The bundle consisted of central 37 heater pins and surrounding 24 dummy pins. The diameter of each pin was 6.5 mm and the pin pitch was 7.9 mm. As concerns the heater pin, the axial heated length was 450 mm and the heat flux was uniform. A spacer wire of 1.3 mm diameter was wrapped around each pin with helical pitch of 265 mm. At nearly middle position of the heated section, a centrally located blockage of 5 mm thickness stainless steel was attached. The blockage covered 36 % of the total flow area.

The pin surface and sodium temperatures were measured by many chromel-alumel thermocouples. All thermocouples were calibrated prior to experiments by checking their outputs at various isothermal conditions. The inlet sodium flow rate was measured by an electromagnetic flow-meter. The output signals from the thermocouples and flow-meter were recorded on a digital data acquisition system.

Operating Procedure

In the first stage where temperature rises were measured under steady-state single-phase conditions, the sodium flow rate and the power level were adjusted to the aimed ones within the following ranges:

Inlet flow velocity	0.50 - 4.07	m/s
Heat flux	4.58 - 94.33	W/cm^2

In the second stage where coolability was examined under quasi-steady-state conditions, the flow rate was initially maintained at the constant value and the heat flux of each pin was adjusted to be aimed one. After steady-state condition was attained, three local boiling steps were conducted by reducing the flow rate. The conditions of boiling experiment were:

Inlet flow velocity	1.46 - 1.08	m/s
Heat flux	61.0	W/cm^2

No dry-out test was conducted with the present 61-pin bundle because of the early failure of heater pins.

SINGLE-PHASE TEST RESULTS AND DISCUSSIONS

Temperature Distributions

Figure 2 shows a typical two-dimensional isotherms of sodium temperature rises behind the blockage. The horizontal and vertical axes represent the subchannel No. and the distance from the blockage, respectively. Here, the three-dimensional distortion effect of spiral wires on the isotherms was eliminated as small as possible by picking up those data which were measured rotationally with wire angle. The dotted points in each subchannel mean the location where the axial temperature distribution curve takes its minimum values. The broken line is, therefore, the envelope of recirculating sodium flow, i.e. the wake region. The shape and size of the wake were not particular to each run but were much the same with many other results, even if the flow velocity was very slow. The isotherms disagreed with recirculating flow patterns and the maximum temperature position appeared again at immediate vicinity of the blockage center[1].

Dimensionless Residence Time

Based on the familiar definition of residence time,

$$\tau = \frac{d_h}{4} c_p \gamma \frac{T_{wk}-T_c}{q'}, \qquad \text{.............................. (1)}$$

we calculated τ for various core flow velocities U_B. The tendency of τ against U_B should be in inverse proportionality, since mean recirculation pass was surely kept constant and the mean recirculation velocity was considered to be proportional to U_B. However, this was not always the case due to the molecular heat conduction for very slowly recirculating sodium behind rather large blockage.

From the insight of the isotherms, we first assumed that the asymptotic value of τU_B ($\propto T_{wk}-T_c$) at high velocity data may be determined cheifly by the heat and mass exchanges through small gaps of only a limited number of pins whose radial locations are just inside of the contour line of blockage. The localized heat and mass exchanges can be considered to extend to a short distance characterized by subchannel diameter d_h rather than whole blockage size D_B. Based on the present assumption, we used not $\tau U_B/D_B$ but $\tau U_B/d_h$ for the dimensionless residence time and examined the analogy of temperature fields observed behind various sizes of blockages. As a natural product of our assumption, we introduced a new dimensionless variable named Ring Parameter. The definition is D_B/p (characteristic length of blockage/pin pitch). The Ring Parameter is correctly proportional to the number of pins around the contour line of blockage when central-type blockages are concerned.

In Fig. 3, the dimensionless residence times are plotted against the Ring Parameter. Almost all data available converged into one line, and was expressed by the empirical formula:

$$\tau U_B/d_h = \frac{c_p \gamma}{4} \frac{U_o}{q'(1-F)} (T_{wk}-T_c) = 35.3(D_B/p)^{0.85}. \qquad \text{......... (2)}$$

The result supported the varidity of our treatment. It will be deduced from this result that the interface area between wake and free stream, where geometrical configuration of triangularly arranged pins plays an important rule for the sodium cross flow, will sheild the long-distance heat and mass transfer. In such a case, major parts of the heat and mass transfer, i.e. the energy balance within the wake, is controlled by the Ring Parameter as formulated in Eq.(2). The power 0.85 on the Ring Parameter can be regarded as the blockage-size dependency of the ratio: (the effective area of heat and mass exchanges) : (the wake volume).

The utilization of the empirical formula was restricted to asmall pin-gap bundle and to small fraction range of blocked flow area. The available data indicates that the formula is effective for the bundles whose subchannel diameters lie within the range $3.0 \leq d_h \leq 16.1$ mm. Similarly, for the fraction of blocked flow area, the restriction becomes $0 \leq F \leq 0.6$ of 169-pin bundle. For very large blockage and large pin-gap configurations, the surrounding pressure field makes the recirculating flow being in abnormally coupled with the core flow(2). This forces our premises into being invalidated.

Extrapolation to Reactor Conditions

The peaking factors, $C_{B,max}=(T_{B,max}-T_c)/(T_{wk}-T_c)$ and $C_w=(T_w-T_c)/(T_B-T_c)$, were obtained, where T_B means an apparent local temperature in the wake that will be observed in case of bare bundle and T_w is the real local temperature under wire-wrapped bundle configuration. From many temperature data measured rotationally at different positions on the same axial location, we estimated that the peaking factor C_w lay from 0.9 to 1.2. The bare bundle peaking factor $C_{B,max}$ was 1.5 to 1.6.

These values were directly multiplied to the estimated wake temperature from Eq.(2). The resultant local temperature rises for the conditions of Japanese prototype reactor MONJU are shown in Fig. 4. In the case of central-type blockage, the local temperature rise first increases with the fraction of the blocked area, and after attaining a 320 °C peak temperature rise at F = 0.3, decreases gradually. The latter tendency, which was similar to that evaluated by Basmer et al. for SNR-300(3), is ascribed to the increase of core flow velocity U_B. It is seen that the central-type blockage will not cause local boiling without being detected by an in-core flow-meter, since the flow-meter can sense the global flow reduction of greater than 10 %. One of the critical conditions of the incipient boiling was the overlapping of the formation of 30 % blockage and the operation under 125 % mismatching of power-to-flow ratio.

BOILING TEST RESULTS AND DISCUSSIONS

Oscillatory Boiling Behavior

Figure 5 shows typical signals observed during the initial non-boiling step of local boiling experiment (Run No. 61WLB-101). The flow velocity was maintained at the constant value of 1.46 m/sec and the heat flux of each pin was adjusted to be 61 W/cm^2. The inlet sodium temperature was 503 °C and the cover gas pressure was 1.01 bar.

In this experiment, three steady-state local boiling steps were conducted under different conditions by reducing the flow velocity stepwise. After the first flow reduction, where the flow velocity was changed to 1.24 m/sec level, the maximum temperature observed within the wake region reached saturation level. Little amounts of initial boiling superheat were identified. During the first step of steady-state local boiling, small vapor bubbles were formed irregularly according to the fluctuation of sodium temperature.

Further reduction of flow velocity caused oscillatory boiling. Figure 6 shows typical signals of inlet velocity, temperatures, pressure and void fraction during the second step of local boiling experiment, where the mean flow velocity was changed to 1.08 m/sec level. During this step, small amount of vapor bubble always survived the oscillation. This conclusion was derived from the attentive interpretation of the present experimental data. The same conclusion has been obtained in the experiments of KfK[4], ECN[5] and PNC[6] (our previous experiments with 37-pin bundle central-type blockage test section). This finding conflicts with the analytical model of oscillatory boiling in which the isothermal compression process of a single bubble is assumed[7]. In other words, total amount of energy transported from bubble to surrounding liquid must be less than the total internal energy of the oscillated bubble: a certain part is originated by the continuous heat input and the other part is worked by the contraction of bubble volume. However, the model brought us contradict answer.

To evaluate more practically the bubble oscillation frequency observed in the present 61-pin and previous 37-pin test bundles, an analytical model has been developed.

The oscillatory behaviors of both liquid and bubble were first formulated by the one dimensional momentum equation of liquid column. Dynamic behavior of liquid column was then expressed by the ordinaly differential equation. In this derivation, linear perturbation method was applied. The bubble behavior was coupled with the displacement of liquid column under the following assumptions:

(1) bubble is represented by a single sphere;
(2) in the process of bubble expansion, vapor pressure is presented by Gast's model (linear temperature profile is assumed within the wake);
(3) in the process of bubble contraction, vapor pressure is presented by polytropic change (i.e. $P_b V^n$=const.).

The experimentally estimated value of mean bubble volume was inputted to the code. The polytropic index was also fixed through the interpretation of measured data. The proper value was 0.1 to 0.2 (for the isothermal and constant pressur compression process menthioned above, "n" equals to 0).

Figure 7 shows the comparison of oscillation frequencies, one was observed in the experiment and another was evaluated from the present code. The horizontal axis means the temperature gradient within the wake. For the derivation of this value, maximum and minimun values of measured temperatures within the wake were used. Concerning the 37-pin bundle results, calculated frequency agreed well with the measured one. However, discrepancy appeared between calculated frequency and measured one in the case of 61-pin bundle.

The tendency of the calculated frequency being higher than the actual one was preparatively examined and its major cause was ascribed to the over-estimation of the used value of temperature gradient. Due to many trouble encountered in the present experiment with 61-pin bundle, we could not obtain enough data to check the reasons of the discrepancy in detail.

Restricting ourselves within rough estimations, we summarized the phenomena of oscillatory boiling and its termination as follows:

(1) oscillatory boiling is stably succeeded when there exists a large difference between the temperatures measured at the wake center and the core flow region;
(2) the oscillation is gradually damped in keeping with the build up of high temperature region around the wake, and at last it will be stabilized (when the coolability is assured).

Dry-out Behavior

Prior to the present 61-pin bundle experiment, dry-out test was conducted with the 37-pin bundle test section (Run No. 37(19)WLB-114). The flow velocity was initially maintained at the constant value of 1.70 m/sec and the heat flux was adjusted to be 167 W/cm^2. The inlet sodium temperature was 461 °C and the cover gas pressure was 1.05 bar.

In this test, the heat flux was increased stepwise with the other conditions being held almost constant. Figure 8 shows the signals observed during the instance of permanent dryout. Horizontal axis means the relative time defined such that the switching off of heater.power can be identified by t = 0 sec.

After the stable oscillatory boiling being succeeded for a long period, the amplitude of osillatory signals became to show damping tendency during the time interval -2 sec to -1 sec in Fig. 8. It was obvious from the experimental data and the analytical estimation curves drawn in Fig. 7 that the gradual growth of radial and axial high temperature region forced the oscillation being stabilized. The main driving force of this behavior was the reduction of the amount of condenced vapor.

As was shown in Fig. 8, pin surface and sodium temperatures measured at the locations both 22 mm downstream of blockage showed steep increases due to the occurrence of dry-out. The sudden one-sided expansion of voiding region was accompanied. The voiding region was, however, limited locally: concerning radial direction, it was extended within about three quarters of blockage diameter, and for axial, it was about three times as long as blockage diameter. The global flow reduction and flow instability were never observed during this dry-out phase. At about 1.5 sec later after the occurence of local dry-out, heater power was cut by detecting local clad melting.

The theoretical excess temperature at the instance of dry-out, which was equal to the temperature rise exceeding saturation temperature and was calculated from simple heat balance equation, was nearly 140 °C. The excess temperature was correlated to the subcooled temperature measured at the axial end of wake region at the instance of boiling inception. Many available data were also refered. The margin to the boiling crisis was found to depend on the subcooled temperature, i.e. a decreasing function of power to flow ratio q'/U_0. It was thus concluded to be sufficiently large for the actual fuel subassembly in compared with our too high q'/U_0 conditions.

CONCLUSION

The succeeding series of central-type blockage experiments were completed The results were summarized as follows:

(1) Single-phase flow

a) The empirical formular was derived to estimate the local temperatur rises behind various central-type blockage.

b) The central-type blocakge will not cause local boiling without being detected by the in-core flow-meter.

(2) Two-phase flow

a) Existance of a large boiling window could be identified.

b) Stable oscillatory boiling improved the coolability of localized bubbly region. Due to this effect, the critical condition of clad melting was expected to be fairly shifted toward that of integral boiling.

These results will be generalized to arbitral type blockages after performing the interpretation of the data that will be derived from our final experiment with 91-pin bundle edge-type blockage test section.

ACKNOWLEDGEMENTS

The authors are indebted to Mr. T. Isozaki and Mr. T. Komaba for their technical contributions to the present experimental work.

NOMENCLATURE

c_p	: Specific heat of sodium	T_c	: Average temperature in core flow
D_B	: Characteristic length of blockage	T_{wk}	: Average temperature in the wake
d_h	: Equivalent diameter of subchannel	U_o	: Inlet flow velocity
F	: Fraction of blocked flow area	U_B	: Flow velocity at unblocked area
P_b	: Bubble pressure	V	: Bubble volume
p	: Pin pitch	τ	: Coolant residence time
q'	: Heat flux	γ	: Specific gravity of sodium

REFERENCES

(1) M. Uotani et al.: "Local Flow Blockage Experiments in 37-pin Sodium Cooled Bundles with Grid Spacers", 8th LMBWG Meeting, Mol (1978)
(2) M. H. Fontana et al.: "Thermal-hydraulic Effects of Partial Blockages in Simulated LMFBR Fuel Assemblies with Application to the CRBR", ORNL-TM-4779 (1975)
(3) P. Basmer et al.: "Experiments on Local Blockages", 6th LMBWG Meeting, Riseley (1975)
(4) F. Huber, W. Peppler: "Form and Development of Boiling behind a 49 % Central Blockage in a 169 Pin Bundle", 7th LMBWG Meeting, (1977)
(5) B. Dorr, J. E. deVries: "The ECN/KfK Local Boiling Experiments in Petten", 8th LMBWG Meeting, Mol (1978)
(6) M. Uotani et al.: "Local Boiling Experiments in a Wire-Wrapped 37-pin Bundle with a Central Blockage", Preprint 1979 Annual Meeting of the Atomic Energy Society of Japan (1979)

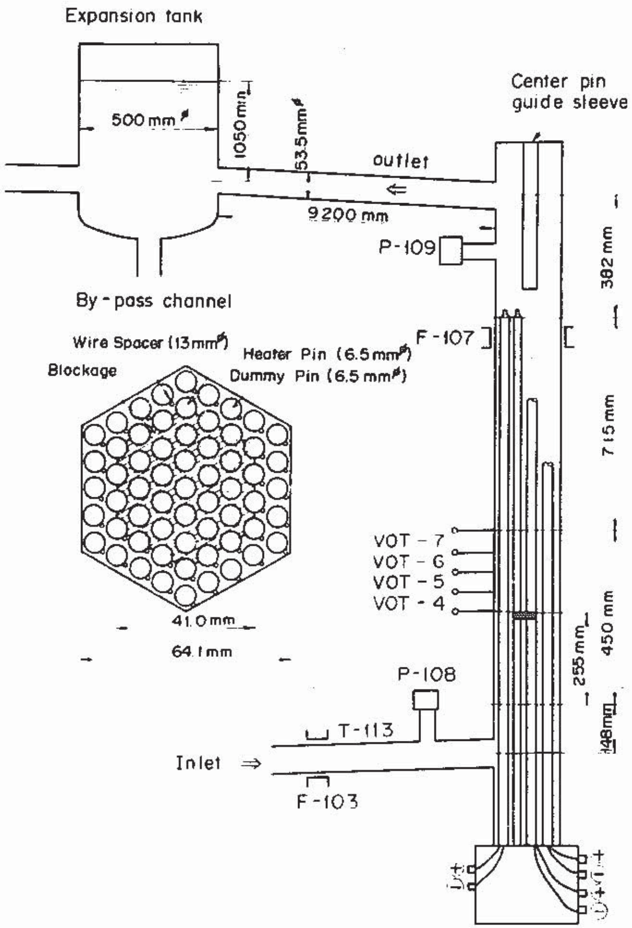

Fig. 1　Locally blocked 61-pin bundle test section　(PNC-FS-1179)

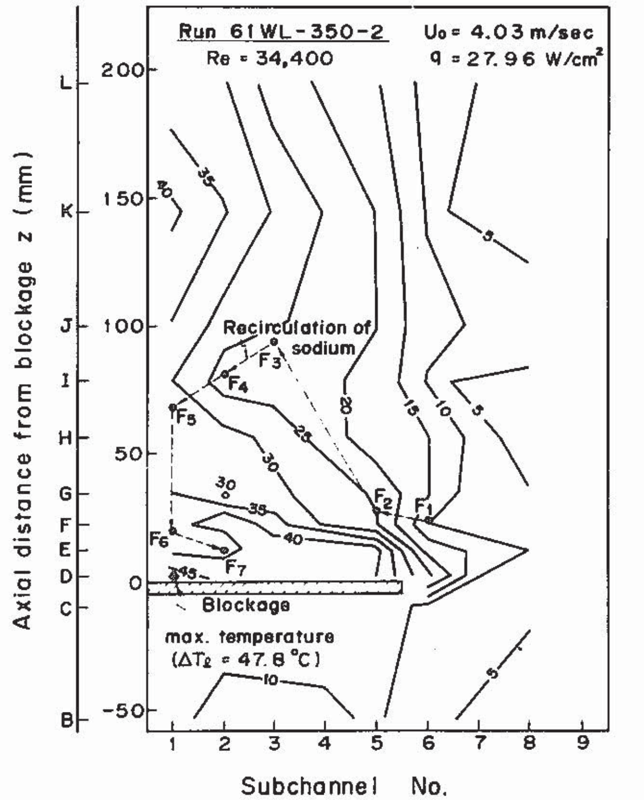

Fig. 2　Isotherms of sodium behind the blockage　(PNC-FS-1086)

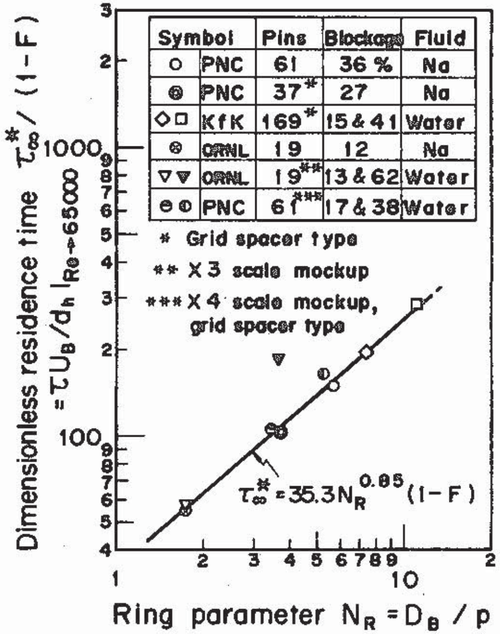

Fig. 3 Correlation between dimensionless residence time and Ring Parameter (PNC-FS-1103)

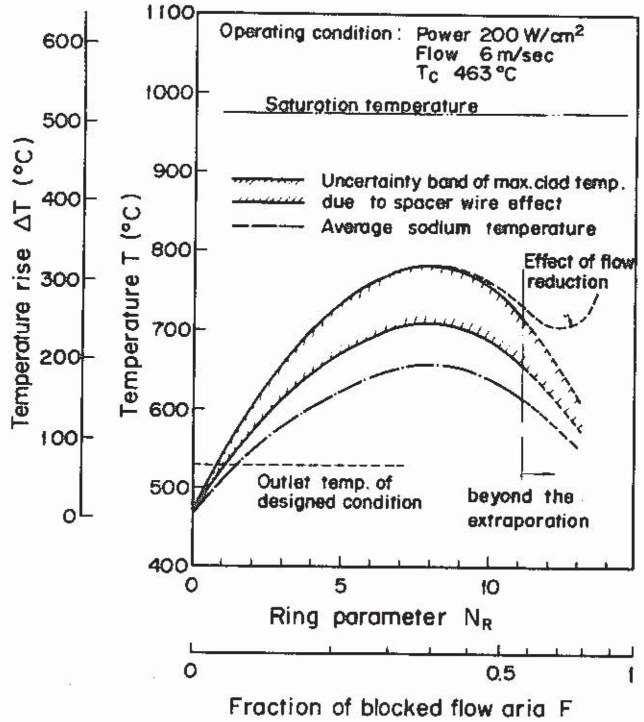

Fig. 4 Estimation of temperature rises behind various blockages, — MONJU condition (PNC-FS-1107)

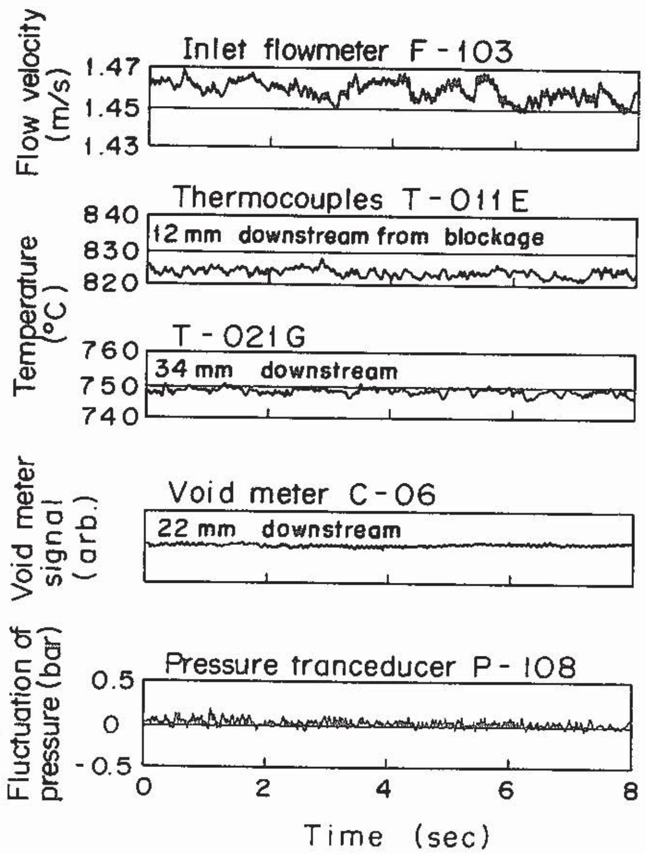

Fig. 5 Signals under non-boiling condition, -- Run No. 61WLB-101 (PNC-FS-1180)

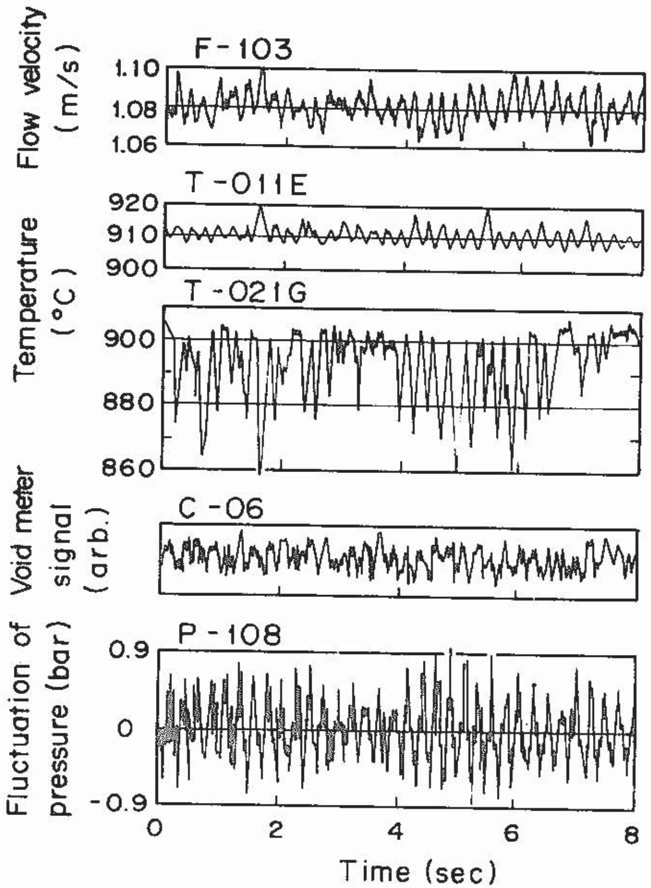

Fig. 6 Signals under oscillatory boiling condition, — Run No. 61WLB-101 (PNC-FS-1181)

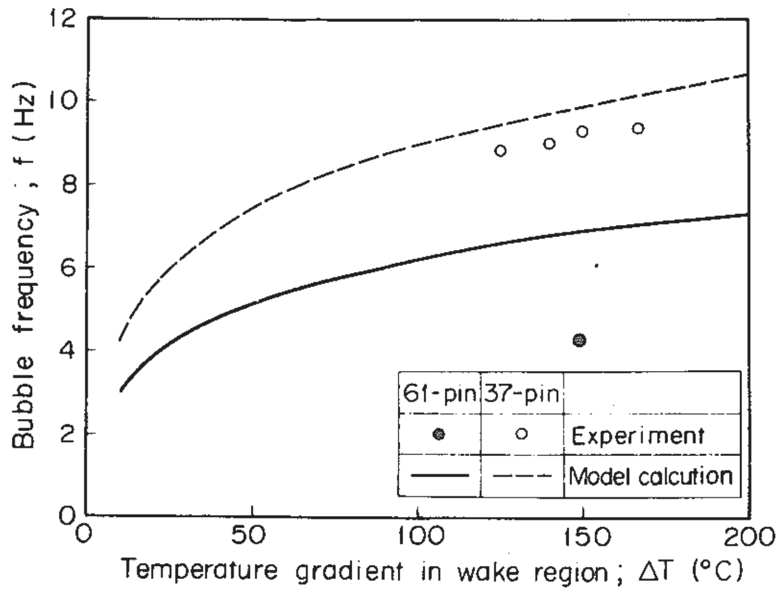

Fig. 7 Effect of temperature gradient in the wake region on the oscillation frefuency (PNC-FS-1188)

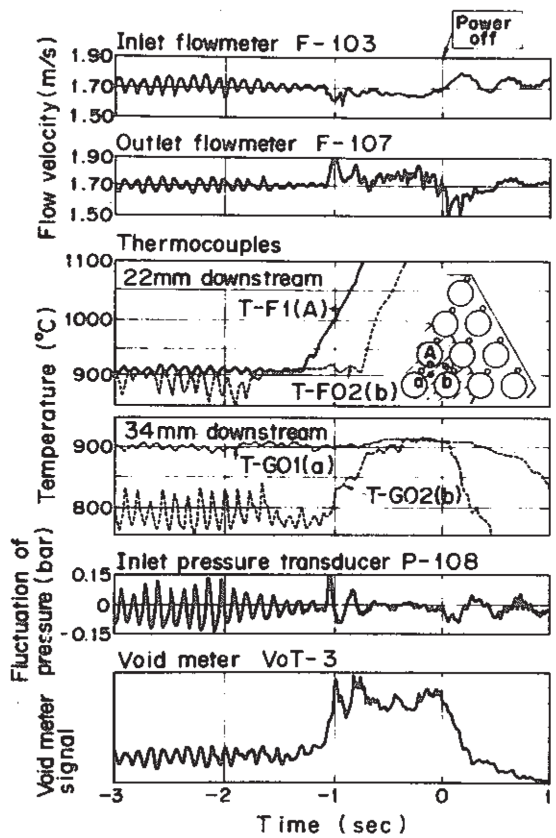

Fig. 8 Signals at the occurrence of permanent dry-out, -- Run No. 37(19)WLB-114 (PNC-FS-1109)